The effect of Sr substitution on superconductivity in $Hg_2(Ba_{1-y}Sr_y)_2YCu_2O_{8-\delta}$: I. A neutron powder diffraction study

2004 J. Phys.: Condens. Matter 16 4061

(http://iopscience.iop.org/0953-8984/16/23/022)

INSTITUTE OF PHYSICS PUBLISHING JOURNAL OF PHYSICS: CONDENSED MATTER

J. Phys.: Condens. Matter **16** (2004) 4061–4076 PII: S0953-8984(04)76651-5

The effect of Sr substitution on superconductivity in $Hg_2(Ba_{1-y}Sr_y)_2YCu_2O_{8-\delta}$: I. A neutron powder diffraction study

P Toulemonde[1,3], P Odier[1], P Bordet[1], S Le Floch[1] and E Suard[2]

[1] Laboratoire de Cristallographie, CNRS, 25 avenue des martyrs, BP166, F-38042 Grenoble cedex 09, France
[2] Institut Laue-Langevin, 6 rue Jules Horowitz, BP156, F-38042 Grenoble cedex 09, France

E-mail: pierre.toulemonde@lpmcn.univ-lyon1.fr

Received 19 February 2004
Published 28 May 2004
Online at stacks.iop.org/JPhysCM/16/4061
DOI: 10.1088/0953-8984/16/23/022

Abstract

The effect of Sr chemical pressure on superconductivity was investigated in $Hg_2(Ba_{1-y}Sr_y)_2YCu_2O_{8-\delta}$. The samples were synthesized at high pressure and high temperature from $y = 0.0$ to full substitution, $y = 1.0$. These Sr substituted compounds are superconducting, without Ca doping on the Y site, and show a T_c increasing with Sr, reaching 42 K for $y = 1.0$. A detailed neutron powder diffraction study compares the structural changes induced by this chemical Sr/Ba substitution and the mechanical pressure effects in the Hg-2212 system. It shows the strong decrease of the three Ba/Sr–O distances and consequently the shrinkage of $Cu–O1_{in-plane}$ and $Cu–O2_{apical}$ bonds. These structural changes, by affecting the charge transfer which occurs between the charge reservoir and the superconducting block, are responsible of the T_c enhancement with Sr content.

(Some figures in this article are in colour only in the electronic version)

1. Introduction

The high pressure–high temperature (HP–HT) process allows one to obtain nearly pure $HgBa_2Ca_{n-1}Cu_nO_{2+2n+\delta}$ mercury based cuprate superconductors, even for $n > 3$ [1, 2]. It is also efficient for the synthesis of the $Hg_2Ba_2YCu_2O_{8-\delta}$ compound (Hg-2212) [3–5]. In $Hg_2Ba_2YCu_2O_{8-\delta}$ a strong oxygen deficiency ($\delta \sim 0.4$–0.5) inhibits superconductivity. Ca^{2+} substitution on the Y^{3+} site in the series $Hg_2Ba_2(Y_{1-x}Ca_x)Cu_2O_{8-\delta}$ restores the

[3] Present address: LPMCN, Université Lyon-I, Bâtiment Léon Brillouin, 43 Boulevard du 11 Novembre 1918, F-69622 Villeurbanne cedex, France.

superconducting state but the Ca solubility limit ($x \sim 0.4$) prevents achieving the optimal doping regime. Thallium (Tl^{3+}) or lead (Pb^{4+}) substitution for Hg^{2+} allows one to extend the Ca solubility domain and to achieve a $T_{c\,max}$ of 82–84 K [6–9].

The Hg-2212 compound shows a giant T_c increase under mechanical pressure, not only for underdoped but also for nearly optimally doped samples: +50 K under 20 GPa [10]. This enhancement is the greatest ever measured in superconducting compounds. In order to stabilize such possible T_c increase at ambient pressure [11–13], 'chemical pressure' was attempted in cuprates by using Sr substitution for Ba. Nevertheless in most cases—except for the La_2CuO_4 system [14–16], where the substitution is not isovalent and changes the doping—the replacement of Ba by Sr produces a continuous decrease of T_c [17–21]. Sr substitution has been already tried in the double-mercury-layer system, but the first attempts lead to an impure Hg-2212 sample accompanied with Hg-1212 [22, 23].

The first aim of this study was to find the optimal experimental conditions for obtaining nearly pure $Hg_2(Ba_{1-y}Sr_y)_2YCu_2O_{8-\delta}$ samples. Then the T_c of these Hg-2212 samples was measured versus Sr content and, surprisingly, an increase of T_c with Sr was observed. The T_c increased from 0 K for the unsubstituted sample ($y = 0$) to 42 K for full substitution ($y = 1.0$). This enhancement was not only observed in the Y based Hg-2212 series but also confirmed in a second Hg-2212 series, doped with 20% of Ca on the Y site, where T_c increases now from 21 K ($y = 0$) to 58–60 K ($y = 0.7$–1.0) [24, 25]. Finally, we performed neutron powder diffraction (NPD) analysis on both series to better determine the origin of this T_c enhancement.

This study is divided in two papers. In this first one, we discuss the structure (from NPD analysis) of two compositions of the Y based series ($y = 0.50$ and 1.0) which were carefully compared with that for $y = 0.0$ [3]. We also compare the effects induced by Sr substitution with those of the mechanical pressure. For that, a second structural information set obtained from refinements of high pressure synchrotron x-ray diffraction patterns was used. These data were acquired during a previous experiment carried out on the high pressure ID-09 beamline at ESRF (European Synchrotron Radiation Facility, Grenoble, France) for a Hg-2212 sample up to 30 GPa using a diamond anvil cell (for more details, see [22, 28]). We conclude that there is a positive chemical pressure effect, showing the structural changes associated with the T_c increase with Sr.

In a second paper [26], we have investigated the charge repartition into the cell by 'bond valence sum' analysis, starting from the structure (determined by NPD analysis). Different origins of a charge transfer to the superconducting CuO_2 plane are identified, which could explain the T_c enhancement with Sr.

2. Experimental details

Two pieces of high pressure equipment were used to synthesize the samples. The first syntheses were carried out using a small belt system (samples of ∼500 mg) to select the best conditions for the HP–HT synthesis. The pressure was kept at 3.5–4 GPa and different time (15–120 min) and temperature (900–1050 °C) conditions were applied. Then, the HP–HT syntheses were carried out in a large volume Conac HP system, with the optimized pressure and temperature conditions, in order to produce larger samples (∼2.4 g) for NPD experiments.

Two different starting mixtures were used; the first one was for selecting the appropriate temperature (T), time (t) and pressure (P) of synthesis to get the purest possible sample. We used the belt apparatus which consumes only a small amount of powder. The powders were prepared by mixing simple oxides HgO (Aldrich, 99%), BaO_2 (Merck, 95%), SrO_2 freshly prepared by precipitation from a nitrate solution of strontium (Aldrich, 99%), Y_2O_3 (Prolabo, 99.9%), CuO (Aldrich, 99%) and metallic Cu (Ventron, 99%) in the appropriate ratio to adjust

the oxygen content. After selecting T, t and P, larger batches were processed for NPD experiments in the Conac HP cell. In this case, we used the second kind of mixture based on precursors of '$(Ba_{1-y}Sr_y)_2YCu_2O_z$' prepared according to the procedure described in [27]. More precisely, for $y = 0.50$, two different precursors '$Ba_2YCu_2O_z$' and '$Sr_2YCu_2O_z$' were prepared by heating the corresponding mixture of oxides at 850 and 950 °C respectively for 24 h. To the precursor(s), HgO was added in the stoichiometric ratio to get the compositions $y = 0.50$ and 1.0. Both samples were prepared at 3.5 GPa and 1050 °C for 60 and 30 min respectively.

T_c was measured by means of the ac susceptibility; this measurement was performed at 119 Hz using a home-made apparatus working at low magnetic field of 0.012 Oe, in the range 4.2–300 K.

The microstructure and composition of samples were investigated by electron microscopy on a Philips CM-300 TEM and JEOL-840 SEM, both equipped with a Kevex system for x-ray energy dispersive spectroscopy (EDX) analysis. In the EDX analysis many regions and grains of the same phase were examined and the compositions averaged. Nevertheless, the EDX composition was calculated without the use of standards (such as Y_2BaCuO_5 and HgS) which would allow a more precise quantification of elements.

X-ray diffraction (XRD) patterns were collected using a powder diffractometer (Siemens D-5000) working in transmission mode at the wavelength $\lambda_{Cu\ K\alpha_1} = 1.540\,56$ Å ($K\alpha_2$ Ni filtered). The neutron powder diffraction experiments were performed at room temperature on the D2B instrument of ILL (Institut Laue-Langevin, Grenoble, France). Each powder sample was introduced into a vanadium can to be supported into the neutron beam. The wavelength was tuned to 1.594 Å and the average collecting time was eight hours which was enough to achieve satisfactory counting statistics. The detector has 64 cells spaced by 2.5° permitting one to record the NPD pattern from $2\theta = 6°$ to 160° with an angular resolution of 0.05°.

3. Results

3.1. Phase composition, unit cell and pressure effect

The purities of samples synthesized in the belt cell or in the Conac HP system are almost identical; they do not depend on the nature of the starting mixture. The main phase is Hg-2212, but sometimes, for Sr rich compositions, Hg-1212 impurity phase is observed due to some reaction with the gold capsule enhanced by the Sr content. To avoid the formation of Hg-1212 phase, the reaction time should be reduced for Sr rich compositions (i.e. from 60 min for $y = 0.5$ to 30 min for $y = 1.0$). Nevertheless, even with optimized time conditions, impurities phases were observed (figure 1): HgO, CuO and an unknown phase whose amount increases with the nominal Sr content. This phase containing Hg, Sr and oxygen has been reported to be $Sr_{0.76}Hg_{1.24}O_2$ according to x-ray diffraction (see the tick marks in the bottom part of figure 1) and EDX data [24, 25]. We assume this phase to have a unit cell close to that of the $Ca_{0.76}Hg_{1.24}O_2$ phase identified in Ca rich (Hg, Pb)-2212 compositions [9] and occurring also in Hg-1223 HP–HT synthesis [29, 30]. The structural model of this $Sr_{0.76}Hg_{1.24}O_z$ impurity (space group $I4/mmm$) will be used to calculate its contribution in the Rietveld refinements (see section 3.4).

Table 1 shows the lattice parameters of our $y = 0.5$ and 1.0 Hg-2212 samples, determined from NPD analysis. They are compared to those for $y = 0.0$ (first column) from Radaelli *et al* [3–5]. A significant and anisotropic decrease of the unit cell is observed: ∼1.3% along the a axis compared to ∼2.7% for c axis. This shows the shrinkage of the lattice due to the progressive replacement of Ba by Sr, with a drop of ∼5% of the unit cell volume. The comparison of the

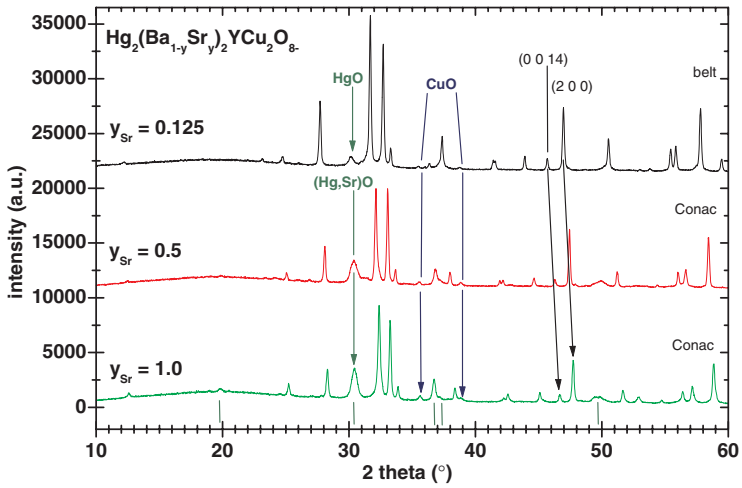

Figure 1. XRD patterns for $Hg_2(Ba_{0.875}Sr_{0.125})_2YCu_2O_{8-\delta}$ (belt synthesis), $Hg_2(Ba_{0.5}Sr_{0.5})_2YCu_2O_{8-\delta}$ and $Hg_2Sr_2YCu_2O_{8-\delta}$ (Conac synthesis) at $\lambda = 1.540\,56$ Å.

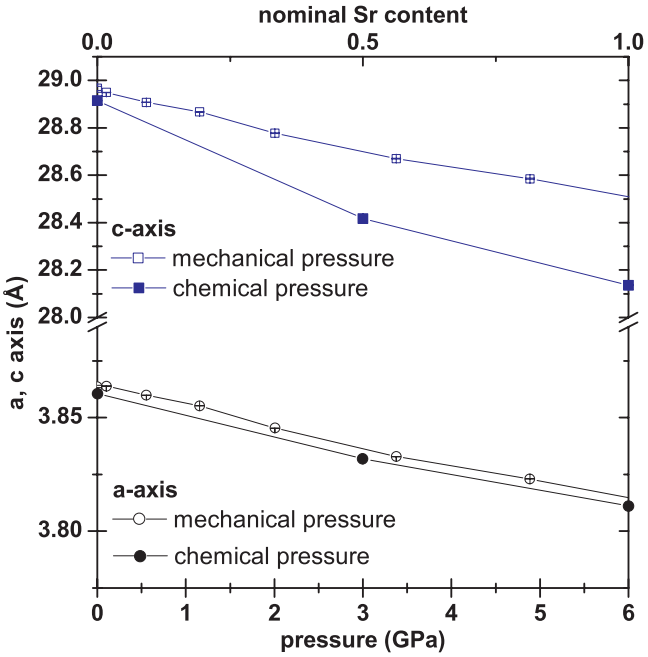

Figure 2. Comparison of chemical and mechanical pressure effects on the lattice parameters in Hg-2212; the *a* and *c* axes are plotted versus nominal Sr content and versus pressure respectively.

a and *c* axis changes with Sr content (upper scale) and with mechanical pressure (lower scale), previously obtained by synchrotron powder diffraction [22, 28], is shown in figure 2. We note that the two effects scale together (illustrated for the *a* axis) suggesting that the substitution of one Ba for one Sr is equivalent to the application of a pressure of ∼6 GPa for the *a* axis and ∼10 GPa for the *c* axis. Nearly identical values were observed by Licci *et al* in the Sr

Table 1. T_c and refined structural parameters from neutron powder diffraction data for $Hg_2Ba_2YCu_2O_{8-\delta}$, $Hg_2(Ba_{0.5}Sr_{0.5})_2YCu_2O_{8-\delta}$ and $Hg_2Sr_2YCu_2O_{8-\delta}$.

Sr content		$y = 0.0$[a]	$y = 0.5$	$y = 1.0$
$a = b$	(Å)	3.8606(1)	3.831 95(5)	3.8112(1)
c	(Å)	28.915(1)	28.4176(7)	28.136(1)
Y	B (Å^2)	0.3(1)	0.74(8)	0.6(1)
Ba/Sr	z	0.1252(2)	0.1266(1)	0.1264(2)
	B (Å^2)	0.5(1)	1.28(9)	1.56(8)
	n (Ba)	1	0.30(5)	—
	n (Sr)	—	0.70(5)	1
Hg/Y	z	0.2126(1)	0.2125(1)	0.2124(1)
	B (Å^2)	1.46(6)	1.98(6)	1.86(7)
	n (Hg)	1	0.83(2)	0.76(2)
	n (Y)	—	0.17(2)	0.24(2)
Cu	z	0.0560(1)	0.0589(1)	0.0592(1)
	B (Å^2)	0.30(6)	0.67(5)	0.32(6)
O1	z	0.0495(1)	0.050 59(8)	0.0517(1)
	B (Å^2)	0.62(6)	0.77(5)	0.71(6)
O2	z	0.1414(3)	0.1403(2)	0.1400(2)
	B (Å^2)	1.5(1)	1.40(7)	1.54(9)
O3	$x = y$	0.574(2)	0.589(2)	0.576(2)
	z	0.2163(4)	0.2150(4)	0.2124(4)
	B (Å^2)	0.7(4)	2.5(3)	1.5(3)
	n	0.78(3)	0.94(2)	0.90(2)
R_{wp} (%)		4.99	4.66	6.04
Bragg R-factor (%)		Not available	7.20	8.31
χ^2		1.070	2.54	3.35
T_c onset (K)		0	32	42

[a] The version of the structure presented here for $y = 0$ is the original model determined by Radaelli *et al* [3–5].

substituted $Y(Ba_{1-x}Sr_x)_2Cu_3O_{7-\delta}$ system (i.e. Cu-1212) [31]. In section 4 we will detail the atomic shifts induced by the 'chemical pressure' and compare them with those observed by mechanical pressure.

3.2. Electron microscopy investigations

A sample of $Hg_2Sr_2YCu_2O_{8-\delta}$ was observed by scanning electron microscopy (SEM) and transmission electron microscopy (TEM). Figure 3 shows its microstructure which is typical of the series. It is composed of well defined platelets 5–10 μm long. The grain size is similar to that obtained for (Hg, Pb)-2212 samples [9, 32]. The composition of the 2212 grains was found to be close to the nominal stoichiometry by EDX analysis. The impurity phase detected by XRD study has also been identified in SEM observations as small grains <1 μm.

In figure 4 we show the electron diffraction (ED) images obtained using two different orientations of typical $Hg_2Sr_2YCu_2O_{8-\delta}$ crystallites. The lattice parameters calculated from these ED images ($a = 3.81$ Å and $c = 28.2$ Å) are consistent with those determined from XRD or NPD patterns. The average composition of several individual crystallites was determined by EDX analysis using a nanoprobe of 20 nm. The composition was '$Hg_{1.42}Sr_{2.22}Y_{1.66}Cu_2O_z$'

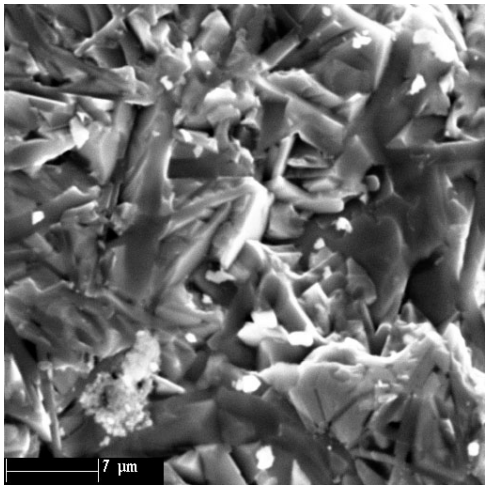

Figure 3. The microstructure of the $y = 1.0$ Sr substituted sample (SEM image).

which can be interpreted as '$(Hg_{0.71}Y_{0.30})_2(Sr_{1.11})_2Y_{1.06}Cu_2O_z$', suggesting the substitution of 30% of Y on the Hg site. This substitution, not taken into account by earlier reports [3–5], was clearly shown in the next studies based on refinements of $Hg_2Ba_2YCu_2O_{8-\delta}$ NPD patterns [22, 24]. This information will be used in our further refinements of the NPD patterns (section 3.4). The 10% excess Sr content might not be representative, being within the error of our EDX estimation.

3.3. Superconducting properties

As shown by ac susceptibility measurements, both samples, with $y = 0.50$ and 1.0, are superconducting (see figure 5 in [25]). This is surprising in view of the absence of superconductivity generally found in $Hg_2Ba_2YCu_2O_{8-\delta}$ [3–5]. Note that in (Hg, Tl)-2212 Tokiwa-Yamamoto *et al* [6] have observed superconductivity at 21 K in the underdoped Tl free compound (superconductivity which disappears after post-annealing in flowing Ar). The superconducting volume fraction shown here (≈35–50%) is high enough to rule out the contribution of another superconducting phase not detected by XRD analysis. As a result, the superconducting transitions at 32 K for $y = 0.5$ and 42 K for $y = 1$ (diamagnetic onset) are unambiguously attributed to the Sr substituted Hg-2212 phase. Hence T_c increases from 0 to 32 K for $y = 0.5$ and 42 K for full substitution. This is the first example in cuprates, except in $(La, Sr)_2CuO_4$ [14–16], or in artificially stressed epitaxial $(La, Sr)_2CuO_4$ films [33], where the Sr substitution raises T_c strongly. The broadening of the transition is probably due to sample inhomogeneities.

As mentioned in the introduction, we have recently confirmed this T_c enhancement with Sr chemical pressure in the Hg-2212 system in a second series, doped with 20% of Ca on the Y site, i.e. with a higher doping level. In this second series, T_c increases from 21 K ($y = 0$) to 58–60 K ($y = 0.7$–1.0) [24, 25]. Thus the phenomenon of T_c increase seems to be intrinsically due to Sr.

3.4. Structure: Rietveld refinements

The structural parameters of $y = 0.5$ and 1.0 samples were refined by the Rietveld method using the software 'Fullprof'. Only the NPD data in the 2θ range 10°–160° were taken into account. The profile shape was calculated on the basis of a pseudo-Voigt function. The

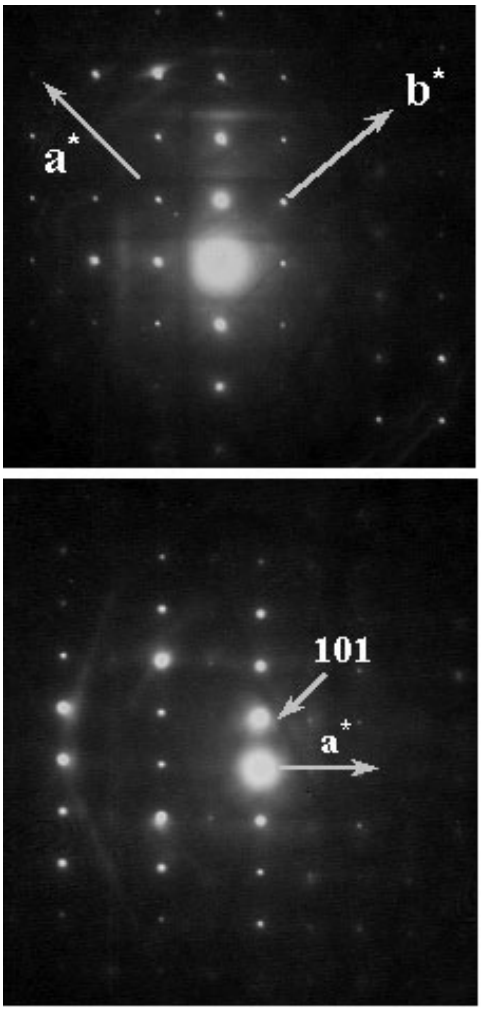

Figure 4. The electron diffraction image in two different orientations of typical crystallites of $Hg_2Sr_2YCu_2O_{8-\delta}$.

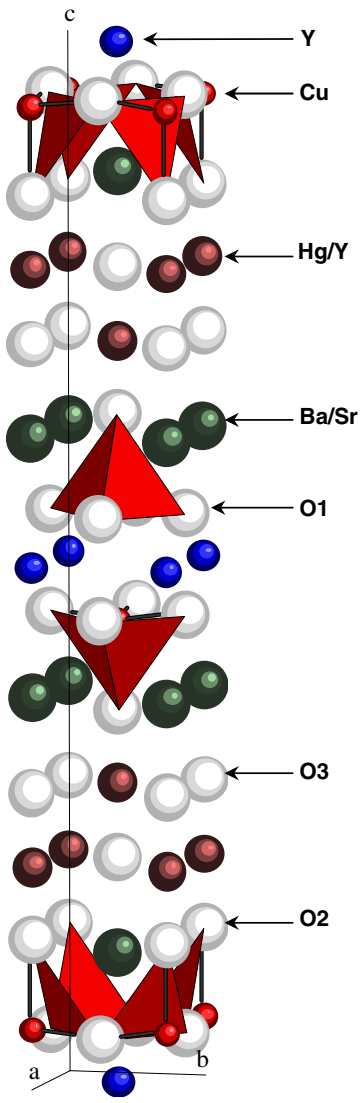

Figure 5. The schematic structure of the Hg-2212 lattice (space group $I/4mmm$) used for NPD Rietveld refinements.

background was approximated by a sixth-order polynomial. The absorption was evaluated and corrected using a cylinder approximation of the sample shape.

The Hg-2212 structure (illustrated in figure 5) was refined on the basis of the tetragonal model (space group $I4/mmm$) previously established for Ba based compounds by Radaelli *et al* [3–5]: Hg/Y at 4e $(0, 0, z \sim 0.21)$, Ba at 4e $(1/2, 1/2, z \sim 0.13)$, Y at 2b $(1/2, 1/2, 0)$, Cu at 4e $(0, 0, z \sim 0.055)$, O1 at 8g $(1/2, 0, z \sim 0.05)$, O2 at 4e $(0, 0, z \sim 0.14)$ and O3 at 4e $(1/2, 1/2, z \sim 0.22)$. The only difference in our calculations consists in taking into account the Sr substitution for Ba but also a possible substitution of Y on Hg sites, as shown by S M Loureiro in $Hg_2Ba_2YCu_2O_{8-\delta}$ [22] and confirmed in our previous work [24]. All the

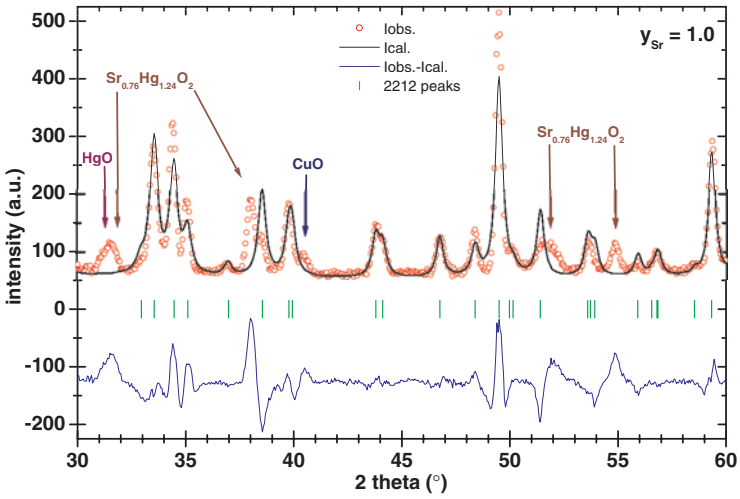

Figure 6. The Rietveld refinement profile of the neutron powder diffraction data ($\lambda = 1.594$ Å) for $Hg_2Sr_2YCu_2O_{8-\delta}$ at room temperature taking into account only the Hg-2212 phase. A difference curve is plotted at the bottom (observed minus calculated). It shows the contribution of HgO, CuO and $Sr_{0.76}Hg_{1.24}O_2$ secondary phases.

Debye–Waller factors were chosen isotropic. We tested anisotropic factors for Hg/Y and O3 sites but they did not improve the refinements.

The secondary phases were taken into account but only their scale factors, lattice parameters and profile shape parameters were refined. Figure 6 shows their contribution to the NPD diffracted intensity in the 2θ range 30°–60°. The merit factors of the refinements were significantly improved by taking into account the HgO and CuO impurities, but also the Sr–Hg–O phase observed from XRD and EDX analysis. The structural model used was that of $Ca_{0.76}Hg_{1.24}O_2$ (space group $I4/mmm$), established previously [30]. In the present case, Ca was assumed to be simply replaced by Sr. We tried also to partially replace Sr by another element (Cu for example), but this partial substitution had no measurable impact on the refined structural parameters (atomic positions or Debye–Waller factors) of the main Hg-2212 phase.

In the starting model, the occupancy factors were supposed to reflect full occupancy. All the thermal Debye–Waller factors converged to reasonable values, except that for O3, in site 4e, which remains close to 5 Å^2, suggesting a non-optimized position of O3 oxygen. This is confirmed by the Fourier difference map calculated from a model without any O3 oxygen (figure 7). It indicates that O3 is displaced from its 4e site towards a neighbouring 16m site. The absence of any additional O4 oxygen on the cell edge (in $(0, y, z)$ sites) of the (Hg, Y)O3 plane was also checked. The position and the occupancy factor of O3 were refined in its 16m (x, x, z) configuration. The final values of the Debye–Waller factors of O3 oxygen did not decrease below 2 Å^2; this indicates the defective character of the (Hg, Y)O3 layer.

The presence of Y substituting for Hg, evidenced by EDX analysis, has been taken into account and the Y/Hg occupancy factor was refined. The difference between the scattering lengths of Y (0.775×10^{-12} cm) and Hg (1.266×10^{-12} cm) was sufficient to allow this calculation.

Among other substitutions, Sr on Y sites would have a strong impact on doping in CuO_2 planes. Unfortunately, NPD would not be useful because of the values of their Fermi lengths being too close ($b = 0.702 \times 10^{-12}$ cm for Sr) for making relevant refinements of the occupancy

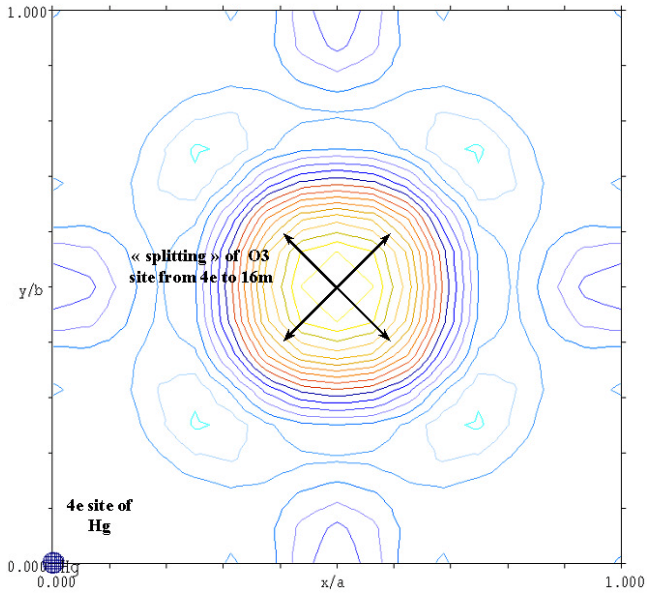

Figure 7. A difference Fourier map ($F_{obs} - F_{calc}$) of the nuclear density generated for the ($x, y, z = 0.2105$) section (i.e. (Hg, Y)O3 plane) of $Hg_2Sr_2YCu_2O_{8-\delta}$. The contribution of the O3 oxygen was omitted from the calculations of F_{calc} to highlight the splitting.

of Y by Sr. However, the large ionic radius difference between Sr^{2+} and Y^{3+} (1.26 Å compared to 1.019 Å with coordination number 8) make the substitution rather improbable. Moreover, in $Hg(Ba, Sr)_2Ca_2Cu_3O_{8+\delta}$ where Ca has the same environment as Y, and where a contrast in values of b between Sr and Ca exists, it was shown that Sr does not substitute at the Ca site [34]. Finally, this substitution is not seen in other cuprates (Cu-1212 [31] or Cu-2212 [35]). We conclude that replacement of Y by Sr is very improbable

It was also possible to refine the Sr content substituting for Ba. A distinct site for Y and Hg in the (Hg, Y)O3 plane was also considered. Both cations could be in 4e, 16m (x, x, z) or 16n (0, y, z) sites, independently or not. Each case was tested but no improvement of the refinement was found. Thus, we chose the simplest case as the most representative one; this is when Y and Hg are on a common 4e site. In figure 8 we show the observed, calculated and difference curves for the $Hg_2(Ba_{0.5}Sr_{0.5})_2YCu_2O_{8-\delta}$ pattern after refinement; there is excellent agreement between the experimental and the calculated profile.

4. Discussion: effects of chemical pressure on the structure

The discussion is organized in two parts. In the first one, we discuss the detailed effects of the Sr substitution on the atomic positions. In doing that, we extract the chemical pressure effect that will be compared to that of the mechanical pressure.

Tables 1 and 2 show the refined parameters for $y = 0.50$ and 1.0. The structure of the $y = 0.0$ compound (unsubstituted), determined by Radaelli *et al* [3–5], has been added for comparison.

The two Sr doped samples ($y = 0.5, 1.0$) have similar refined O3 occupancies (0.94(2) and 0.90(2) respectively), i.e. close to one. This nearly full O3 occupancy is a consequence of the presence of Y^{3+} substituting for Hg^{2+} (17% and 24% for $y = 0.5$ and 1.0 respectively; table 1),

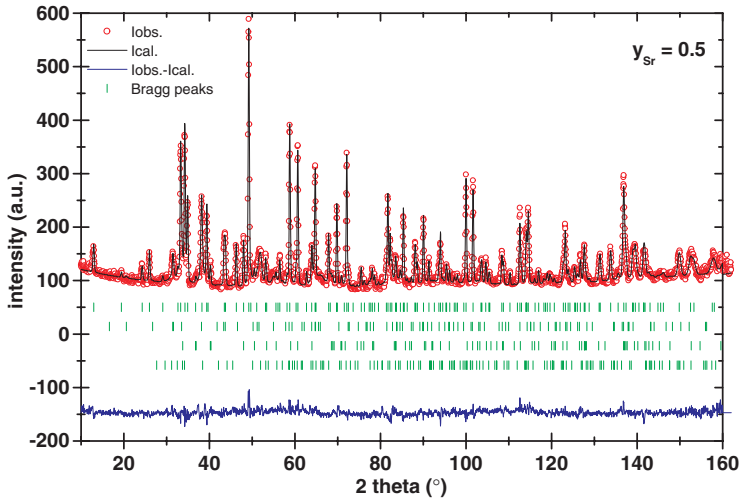

Figure 8. The Rietveld refinement profile of the NPD data ($\lambda = 1.594$ Å) for $Hg_2(Ba_{0.5}Sr_{0.5})_2YCu_2O_{8-\delta}$ at room temperature. A difference curve is plotted at the bottom (observed minus calculated). Tick marks correspond to Bragg peaks of the Hg-2212 phase, $Sr_{0.76}Hg_{1.24}O_2$, CuO and HgO.

Table 2. Selected interatomic distances (in Å) and bond angles (in degrees) for $Hg_2Ba_2YCu_2O_{8-\delta}$ [3–5], $Hg_2(Ba_{0.5}Sr_{0.5})_2YCu_2O_{8-\delta}$ and $Hg_2Sr_2YCu_2O_{8-\delta}$ as obtained from Rietveld refinement of NPD data.

Sr content	$y = 0.0$	$y = 0.5$	$y = 1.0$
Y–O1	2.403(2)	2.395(1)	2.398(2)
Ba/Sr–O2	2.770(2)	2.737(9)	2.722(1)
Ba/Sr–O1	2.919(5)	2.888(3)	2.836(4)
Ba/Sr–O3	2.66(1)	2.56(1)	2.46(1)
Cu–O1	1.9396(5)	1.9305(5)	1.9173(5)
Cu–O2	2.469(9)	2.312(6)	2.272(8)
Hg/Y–O2	2.057(7)	2.052(6)	2.038(7)
Hg/Y–O3[a]	2.10(1)	2.116(1)	2.15(1)
Hg/Y–O3[b]	2.328(9)	2.231(6)	2.284(6)
Hg/Y–O3[b]	2.762(2)	2.753(7)	2.726(6)
Hg/Y–O3[b]	3.136(9)	3.190(6)	3.106(6)
Cu–O1–Cu	168.8(3)	165.95(2)	167.33(2)

[a] Vertical.
[b] In-plane.

filling oxygen vacancies in the (Hg, Y)O3 plane. The presence of Y on the Hg site agrees with SEM data with a refined value, 0.17(2) for $y = 0.50$ and 0.24(2) for the $y = 1.0$ sample respectively, that is close to that deduced from EDX analysis ($\approx$0.30 for the $y = 1.0$ sample). Let us recall that Loureiro [22] also refined the original NPD data for $y = 0.0$ of Radaelli *et al* [3–5] using a rather complex model. His conclusion tends to prove that Y substitutes partially (13%) at the Hg site and provides a high occupancy of O3 (0.88(1) instead of 0.78(3), i.e. corresponding to the oxygen composition O7.76). We have confirmed this suggestion by synthesizing $(Hg_{0.85}Y_{0.15})_2Ba_2YCu_2O_8$ (nominal composition) [24]. The refinement of the

Y occupancy on the Hg site from NPD data gives a value of 21% that is consistent with the synthesis. Thus, the O3 occupancy for $y = 0.5$ and 1.0 compositions is finally close to that of a pure Ba based sample: 0.88(1), as recalculated by Loureiro. The refined occupancy factor of Sr for the $y = 0.50$ sample, 0.70(5), is probably overestimated.

From the refined compositions (O3 and Y/Hg occupancies), one can calculate the formal copper valence; one obtains 2.13 (with 13% of Y on the Hg site and $n(O3) = 0.88$), 2.21 and 2.06 respectively for $y = 0.0$, 0.5 and 1.0. No coherent correlation between this Cu valence (correlated with small oxygen content variations around $O_{7.76}-O_{7.88}$ and the partial Y content on the Hg site) and the continuous increase of T_c can be found. Moreover, as shown by Alonso *et al* [36], a simple formal valence analysis is not appropriate in the case of Hg-2212. The doping level of the CuO_2 planes should be lower than expected from ionic considerations.

Figure 9 shows the effect of the Sr (nominal) content on the z coordinate of the different atomic sites. The graphs are stacked vertically as in the real structure with the same scale for direct comparison. The total variation 'Δz' is indicated on the figure. Although the refined positions are close to those of the original 2212 model without strontium, some changes are clearly observed. The most striking effect concerns Cu and O1 atoms of the superconducting block 'SB' (composed of the two CuO_2 superconducting planes separated by the Y plane) whose z coordinates increase respectively by 3.2×10^{-3} and 2.2×10^{-3} when the Sr content increases from $y = 0$ to 1. This change has no effect on the buckling angle of the superconducting planes which remains close to $\sim 13°$–$14°$ (table 2) while the cell shrinks significantly. The other atoms (Ba/Sr, O2, Hg/Y) do not move more than 1.4×10^{-3}. The O3 oxygen of the (Hg, Y)O3 plane is displaced towards the Hg/Y plane by 3.9×10^{-3}, making the (Hg/Y)O3 plane flat. At the same time, the O3 atom shifts in the direction of the Ba/Sr site and, consequently, the (Ba/Sr)–O3 bond length decreases.

The modifications of the '$(Hg/Y)O_6$', '$(Ba/Sr)O_9$', 'YO_8' and 'CuO_5' coordination polyhedra are illustrated in figure 10 with the same scale. The principal effect is observed for the three neighbouring oxygens, O1, O2 and O3, of the Ba/Sr site which become closer (along the c axis) to the Ba/Sr site, as a consequence of its smaller mean ionic radius. However the shrinkage is not isotropic. The most significant change concerns O3 atoms that become 7.7% closer to Ba/Sr while Ba/Sr–O1 shrinks by 2.8% and Ba/Sr–O2 only by 1.7% (Ba/Sr and O2 are located at approximately the same z). It is then obvious that the distance connecting the SB together decreases significantly. Here, the chemical pressure does not mimic the mechanical pressure of 1 GPa which compresses Ba–O1, lets Ba–O2 remain unchanged and extends Ba–O3 bonds in Hg-2212 (NPD data) [22, 28]. In the one-Hg-layer family, the compressibility of bonds is extremely sensitive to the doping level, i.e. the O3 oxygen concentration in the mercury plane. The behaviour of Ba–O bonds in our Sr substituted Hg-2212 is close to that observed in overdoped Hg-1201 under mechanical pressure [37, 38].

The influences of Sr substitution, i.e. 'chemical pressure', are not restricted to the Ba/Sr site; they extend beyond, up to the Cu site. The distance Cu–O2 (apical) is the bond most significantly renormalized by the Sr substitution. It amounts to a total shrinkage of 8% (for $y = 1.0$). The Cu–O2 distance becomes very small, i.e. 2.27 Å, compared to the value found in Hg-12 $(n-1)n$, i.e. 2.75–2.80 Å [38–40]. This should affect the charge distribution and particularly the charge transfer from the charge reservoir 'CR' (composed by the double (Hg/Y)O3 layer, linked to its two neighbouring Ba/SrO2 planes) to the SB. In agreement, such a decrease is also observed in Hg-12 $(n-1)n$ when holes are injected in the superconducting plane by oxygen doping [41, 42], but also in $(La_{1-x}Ca_x)(Ba_{1.75-x}La_{0.25+x})Cu_3O_y$ where moreover a maximum of the buckling angle occurs exactly at $T_{c\ max}$ [43]. However, for $n = 1$, it has been demonstrated (see references in [38]) by fluorination that Cu–O2 distance reduction does not cause an enhancement of T_c; it is more likely the compression of the in-plane Cu–O1

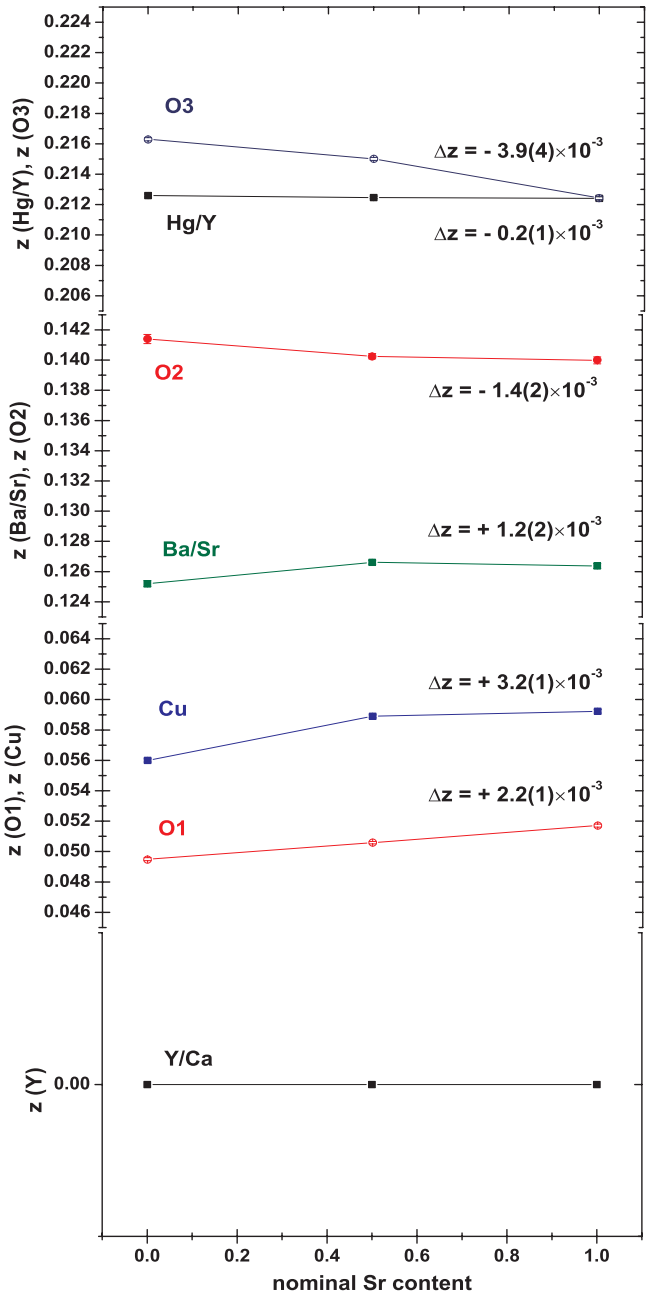

Figure 9. z positions of atomic sites in $Hg_2Ba_2YCu_2O_{8-\delta}$ [3–5], $Hg_2(Ba_{0.5}Sr_{0.5})_2YCu_2O_{8-\delta}$ and $Hg_2Sr_2YCu_2O_{8-\delta}$ as a function of the nominal Sr content.

distance that is responsible for the T_c enhancement. This proceeds in the same way as that observed for strained films. In-plane compressive strain in epitaxial $La_{1.9}Sr_{0.1}CuO_4$ thin films induces a doubling of T_c from 25 to 49 K while the a axis (and thus the Cu–O1 distance) decreases from 3.784 Å (bulk) to 3.76 Å [33], giving $dT_c/da \approx 1000$ K Å^{-1}. In our Sr substituted Hg-2212 samples, Cu–O1 shrinks by only 1.2%; that is small, but follows the trend. Interestingly, the corresponding T_c increase rate reaches $42/(3.8606 - 3.8112) \approx 850$ K Å^{-1}.

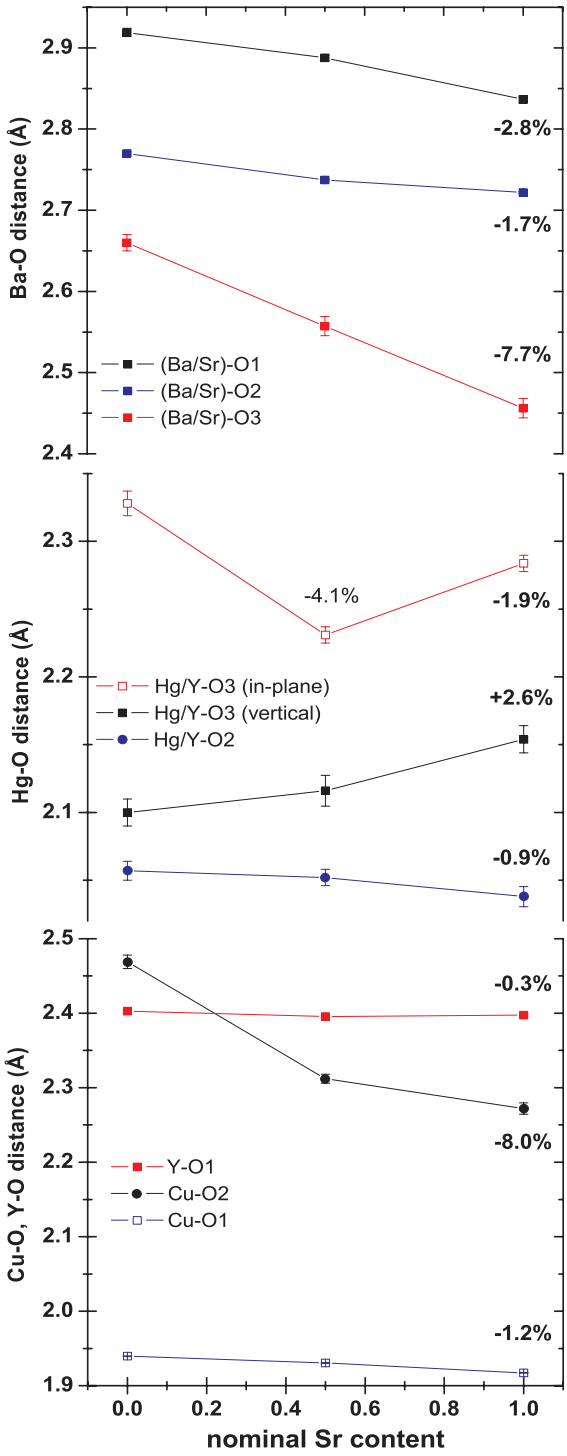

Figure 10. Interatomic distances (in Å) for $Hg_2Ba_2YCu_2O_{8-\delta}$ [3–5], $Hg_2(Ba_{0.5}Sr_{0.5})_2YCu_2O_{8-\delta}$ and $Hg_2Sr_2YCu_2O_{8-\delta}$ samples as a function of the nominal Sr content. The label indicates the total shrinkage in %.

In contrast, the Hg/Y–O2 distance shows smaller relative variation, less than 1%. This is consistent with the smaller compressibility observed for the Hg–O2 bond in Hg-1201 [44].

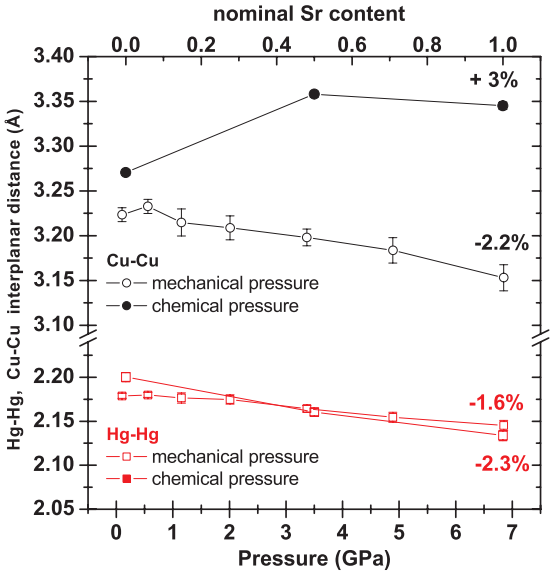

Figure 11. Comparison of chemical and mechanical pressure effects on the internal SB and CR thickness in Hg-2212: Cu–Cu and Hg–Hg distances versus nominal Sr content and versus pressure.

Along the z axis, O3 moves away from Hg/Y, increasing the distance Hg/Y–O3 (between two adjacent Hg/YO3 planes) by 2.6%, which is similar to the decrease of the (Ba/Sr)–O1 distance. This is the second highest effect, after the shrinkage of (Ba/Sr)–O3. The variation of the in-plane Hg/Y–O3 distance, highly sensitive to the small changes of the Y content on the Hg site, is not continuous and therefore cannot be correlated with the T_c enhancement.

It is now interesting to compare the effects of chemical pressure and mechanical pressure [22, 28]. The chemical pressure for $y = 1.0$ is equivalent to a mechanical pressure of 6 GPa approximately, as stated in section 3.1. We will restrict the analysis to pressures lower than 7 GPa. Figures 11 and 12, compare the variations of the CR and SB thicknesses and Hg–Hg and Cu–Cu distances, for chemical pressure (NPD data) and mechanical pressure (synchrotron data). They are similar, except one feature: the Cu–Cu distance which quantifies the SB thickness. It increases by 3% with Sr substitution, but decreases by 2% on applying mechanical pressure. The same effect is observed in the monolayer (Hg, Re)-1223 family: the complete substitution of Sr increases the SB thickness by 3% [45, 46]. The same trend is also observed in the $Cu_2(Ba_{1-x}Sr_x)_2YCu_2O_8$ [35] and $Cu(Ba_{1-x}Sr_x)_2YCu_2O_{7-\delta}$ [31] compounds. This increase is then intrinsic to the presence of Sr; it cannot be related to T_c which increases with Sr substitution in Hg-2212 while it decreases in the latter compounds. At the same time, the interplanar Ba–SB–Ba thickness decreases drastically by 3–4%. Then, the BaO2 and CuO1 planes move towards each other, which leads to a great decrease of the apical Cu–O2 distance to 2.27 Å. The variation of the Hg–Hg distance (−2.3%) follows the variation of the Ba–CR–Ba thickness which decreases by about 2%.

5. Conclusion

The structural effect of chemical pressure in $Hg_2(Ba_{1-y}Sr_y)_2YCu_2O_{8-\delta}$ was studied by means of neutron powder diffraction and correlated with the superconducting properties. The Sr substitution in Hg-2212 has a positive effect on T_c in contrast to the case for the majority of cuprates. It gradually increases T_c from 0 K ($y = 0.0$) to 42 K ($y = 1.0$). Moreover the Sr substituted compounds are already superconducting without Ca doping on the Y site. No

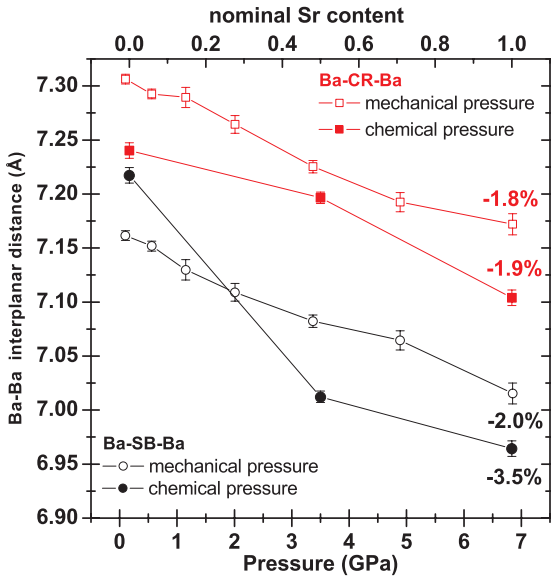

Figure 12. Comparison of chemical and mechanical pressure effects on the external SB and CR thickness in Hg-2212: Ba–SB–Ba and Ba–CR–Ba distances versus nominal Sr content and versus pressure.

coherent correlation can be made between the continuous T_c increase and the variation of the formal valence of Cu in the Sr substituted series.

From a structural point of view, the chemical pressure introduced by Sr is similar to the mechanical pressure, except for the SB thickness which increases with Sr substitution while it decreases under external pressure. However, this is not correlated with the variation of T_c, as proved by the comparison with Hg-1223, Cu-1212 or Cu-2212 systems. The detailed analysis of the atomic positions shows a shrinkage of the '$(Ba/Sr)O_9$' coordination polyhedra with the Sr content, i.e. a strong decrease of the Ba/Sr–O(1)(2)(3) bonds. As a consequence, Cu–O1 and Ba/Sr–O2 planes become closer, but no effect on the Y–O1 bonds (i.e. between the CuO_2 superconducting planes) is observed. The Sr chemical pressure has a pronounced effect on the Hg/Y–O3 bond which increases, making the Hg/Y–O bond flat, while it strongly decreases the $Cu–O1_{in-plane}$ and $Cu–O2_{apical}$ bonds. These structural changes, particularly the last two, should greatly affect the charge repartition in the 2212 lattice and thus the charge transfer towards the superconducting planes, explaining the observed T_c increase with Sr content. This aspect will be developed in part II of this article using a 'bond valence sum' approach.

Acknowledgments

P Toulemonde thanks CNRS for financial support during PhD research. The authors acknowledge R Argoud, C Brachet and R Bruyère for technical assistance in HP–HT experiments. The authors are grateful for stimulating discussions with Dr J L Tholence and for his help in measuring the ac susceptibilities.

References

[1] Capponi J J, Kopnin E M, Loureiro S M, Antipov E V, Gautier E, Chaillout C, Souletie B, Brunner M, Tholence J L and Marezio M 1996 *Physica* C **256** 1
[2] Loureiro S M, Antipov E V, Kopnin E M, Brunner M, Capponi J J and Marezio M 1996 *Physica* C **257** 117
[3] Radaelli P G, Marezio M, Perroux M, de Brion S, Tholence J L, Huang Q and Santoro A 1994 *Science* **265** 380

[4] Radaelli P G, Marezio M, Tholence J L, de Brion S, Loureiro S, Santoro A, Huang Q, Capponi J J, Alario-Franco M and Chaillout C 1994 *Physica* C **235–240** 925
[5] Radaelli P G, Marezio M, Tholence J L, de Brion S, Santoro A, Huang Q, Capponi J J, Chaillout C, Krekels T and Tendeloo G V 1995 *J. Phys. Chem. Solids* **56** 1471
[6] Tokiwa-Yamamoto A, Tatsuki T, Wu X-J, Adachi S and Tanabe K 1996 *Physica* C **259** 36
[7] Toulemonde P, Bordet P, Capponi J J, Tholence J L and Odier P 1999 *Applied Superconductivity* (*Inst. Phys. Conf. Ser.* vol 167) p 271
[8] Toulemonde P, Sin A, Bordet P, Tholence J L and Odier P 2000 *Physica* C **341–348** 677
[9] Toulemonde P, Odier P, Bordet P, Bruyère R and Tholence J L 2002 *Physica* C **366** 147
[10] Acha C, Loureiro S M, Chaillout C, Tholence J L, Capponi J J, Marezio M and Nunez-Regueiro M 1997 *Solid State Commun.* **102** 1
[11] Marezio M and Licci F 2000 *Supercond. Sci. Technol.* **13** 451
[12] Marezio M, Licci F and Gauzzi A 2000 *Physica* C **337** 195
[13] Marezio M, Gilioli E, Radaelli P G and Licci F 2000 *Physica* C **341–348** 375
[14] Cava R J, van Dover R B, Batlogg B and Rietman E A 1987 *Phys. Rev. Lett.* **58** 408
[15] Torrance J B, Tokura Y, Nazzal A I, Bezinge A, Huang T C and Parkin S S P 1988 *Phys. Rev. Lett.* **61** 1127
[16] Radaelli P G, Hinks D G, Mitchell A W, Hunter B A, Wagner J L, Dabrowski B, Vandervoort K G, Viswanathan H K and Jorgensen J D 1994 *Phys. Rev.* B **49** 4163
[17] Wada T, Adachi S, Mihara T and Inaba R 1987 *Japan. J. Appl. Phys.* 2 **26** L706
[18] Ganguli A K and Subramanian M A 1991 *J. Solid State Chem.* **90** 382
[19] Subramanian M A and Whangbo M H 1993 *J. Solid State Chem.* **109** 410
[20] Karpinski J, Schwer H, Kazakov S M, Angst M, Jun J, Wisniewksi A and Puzniak R 2000 *Physica* C **341–348** 421
[21] Sin A, Alsina F, Mestres N, Sulpice A, Odier P and Núñez-Regureiro M 2001 *J. Solid State Chem.* **161** 355
[22] Loureiro S M 1997 *PhD Thesis* Grenoble, France
[23] Chaillout C, Loureiro S M, Toulemonde P, Capponi J J and Marezio M 1997 *Physica* C **282–287** 895
[24] Toulemonde P 2000 *PhD Thesis* Grenoble, France
[25] Toulemonde P and Odier P 2004 *Physica* C **402** 152
[26] Toulemonde P, Odier P, Bordet P, Le Floch S and Suard E 2004 *J. Phys.: Condens. Matter* **23** 4077
[27] Toulemonde P, Le Floch S, Bordet P, Capponi J J, Mézouar M and Odier P 2000 *Supercond. Sci. Technol.* **13** 1129
[28] Bordet P, Loureiro S M, Capponi J J and Radaelli P G 1997 *17th European Crystallographic Mtg*
[29] Le Floch S, Mézouar M, Antérion B, Toulemonde P, Prat A, Bougerol-Chaillout C and Bordet P 2000 *AIRAPT-17: Proc. Science and Technology of High Pressure* vol 2, ed M H Manghnani, W J Nellis and M F Nicol, p 726
[30] Bordet P, Le Floch S, Bougerol-Chaillout C, Prat A, Antérion B and Mézouar M 2000 *Physica* C **341–348** 577
[31] Licci F, Gauzzi A, Marezio M, Radaelli P, Masini R and Chaillout-Bougerol C 1998 *Phys. Rev.* B **58** 15208
[32] Toulemonde P, Odier P, Bordet P, Brachet C and Suard E 2002 *Physica* C **377** 146
[33] Locquet J-P, Perret J, Fompeyrine J, Mächler E, Seo J W and Van Tendeloo G 1998 *Nature* **394** 453
[34] Chmaissem O, Jorgensen J D, Yamaura K, Hiroï Z, Takano M, Shimoyama J and Kishio K 1996 *Phys. Rev.* B **53** 14647
[35] Karpinski J, Kazakov S M, Angst M, Mironov A, Mali M and Roos J 2001 *Phys. Rev.* B **64** 094518
[36] Alonso R E, Rodriguez C O and Christensen N E 2001 *Phys. Rev.* B **63** 134506
[37] Balagurov A M, Sheptyakov D V, Aksenov V L, Antipov E V, Putilin S N, Radaelli P G and Marezio M 1999 *Phys. Rev.* B **59** 7209
[38] Antipov E V, Abakumov A M and Putilin S N 2002 *Supercond. Sci. Technol.* **15** R31
[39] Radaelli P G, Wagner J L, Hunter B A, Beno M A, Knapp G S, Jorgensen J D and Hinks D G 1993 *Physica* C **216** 29
[40] Chmaissem O, Huang Q, Antipov Q E V, Putilin S N, Marezio M, Loureiro S M, Capponi J J, Tholence J L and Santoro A 1993 *Physica* C **217** 265
[41] Wagner J L, Hunter B A, Hinks D G and Jorgensen J D 1995 *Phys. Rev.* **51** 15407
[42] Aksenov V L, Balagurov A M, Sikolenko V V, Simkin V G, Alyoshin V A, Antipov E V, Gippius A A, Mikhailova D A, Putilin S N and Bouree F 1997 *Phys. Rev.* B **55** 3966
[43] Chmaissem O, Jorgensen J D, Short S, Knizhnik A, Eckstein Y and Shaked H 1999 *Nature* **397** 45
[44] Hunter B A, Jorgensen J D, Wagner J L, Radaelli P G, Hinks D G, Shaked H and Hittermand R L 1994 *Physica* C **221** 1
[45] Armstrong A R, David W I F, Gameson I, Edwards P P, Capponi J J, Bordet P and Marezio M 1995 *Phys. Rev.* B **52** 15551
[46] Marezio M and Licci F 1997 *Physica* C **282–287** 53